ResearchGate

See discussions, stats, and author profiles for this publication at: https://www.researchgate.net/publication/274258909

In Silico and in Vitro Study of Binding Affinity of Tripeptides to Amyloid Beta Fibrils: Implications for Alzheimer's Disease.

ARTICLE *in* THE JOURNAL OF PHYSICAL CHEMISTRY B · MARCH 2015

Impact Factor: 3.3 · DOI: 10.1021/acs.jpcb.5b00006 · Source: PubMed

READS

67

7 AUTHORS, INCLUDING:

Man Hoang viet

North Carolina State University

19 PUBLICATIONS **146** CITATIONS

SEE PROFILE

Zuzana Bednarikova

Institute of Experimental Physics SAS

11 PUBLICATIONS **16** CITATIONS

SEE PROFILE

Zuzana Gazova

Institute of Experimental Physics SAS

38 PUBLICATIONS **651** CITATIONS

SEE PROFILE

Mai Suan Li

Institute of Physics of the Polish Academy of S…

154 PUBLICATIONS **2,014** CITATIONS

SEE PROFILE

Available from: Man Hoang viet

Retrieved on: 02 February 2016

THE JOURNAL OF PHYSICAL CHEMISTRY B

Article

pubs.acs.org/JPCB

In Silico and *in Vitro* Study of Binding Affinity of Tripeptides to Amyloid β Fibrils: Implications for Alzheimer's Disease

Man Hoang Viet,[†,‡] Katarina Siposova,[⊥,§,‡] Zuzana Bednarikova,[⊥,§] Andrea Antosova,[⊥,§] Truc Trang Nguyen,[∥] Zuzana Gazova,*[,⊥] and Mai Suan Li*[,†]

[†]Institute of Physics, Polish Academy of Sciences, Al. Lotnikow 32/46, 02-668 Warsaw, Poland

[⊥]Department of Biophysics, Institute of Experimental Physics, Slovak Academy of Sciences, Watsonova 47, 040 01 Kosice, Slovakia

[§]Department of Biochemistry, Institute of Chemistry, Faculty of Science, P. J. Safarik University, Srobarova 2, 041 54 Kosice, Slovakia

[∥]Institute for Computational Science and Technology, Quang Trung Software City, Tan Chanh Hiep Ward, District 12, Ho Chi Minh City, Vietnam

Supporting Information

ABSTRACT: Self-assembly of Aβ peptides into amyloid aggregates has been suggested as the major cause of Alzheimer's disease (AD). Nowadays, there is no medication for AD, but experimental data indicate that reversion of the process of amyloid aggregation reduces the symptoms of disease. In this paper, all 8000 tripeptides were studied for their ability to destroy Aβ fibrils. The docking method and the more sophisticated MM-PBSA (molecular mechanics Poisson−Boltzmann surface area) method were employed to calculate the binding affinity and mode of tripeptides to Aβ fibrils. The ability of these peptides to depolymerize Aβ fibrils was also investigated experimentally using atomic force microscopy and fluorescence spectroscopy (Thioflavin T assay). It was shown that tripeptides prefer to bind to hydrophobic regions of $6A\beta_{9-40}$ fibrils. Tripeptides WWW, WWP, WPW and PWW were found to be the most potent binders. *In vitro* experiments showed that tight-binding tripeptides have significant depolymerizing activities and their DC_{50} values determined from dose−response curves were in micromolar range. The ability of nonbinding (GAM, AAM) and weak-binding (IVL and VLA) tripeptides to destroy Aβ fibrils was negligible. *In vitro* data of tripeptide depolymerizing activities support the predictions obtained by molecular docking and all-atom simulation methods. Our results suggest that presence of multiple complexes of heterocycles forming by tryptophan and proline residues in tripeptides is crucial for their tight binding to Aβ fibrils as well as for extensive fibril depolymerization. We recommend PWW for further studies as it has the lowest experimental binding constant.

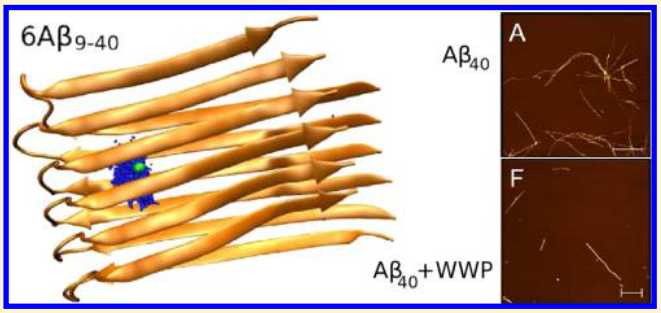

INTRODUCTION

AD (Alzheimer's disease) is a frequent type of dementia, and the number of cases is substantially growing with population age.[1] The patients suffering from AD will see a reduced memory[2] and deteriorating language[3] and will have problems with visual as well as spatial search[4] *etc.* This disease is presumably defined by a gradual accumulation of amyloid deposits consisting τ-protein[5] or Aβ peptides.[6] The hypothesis about amyloid aggregation as a reason for AD is strongly supported by genetic and pathological evidence.[7,8] Aβ peptides are produced by proteolytic cleavage of APP (amyloid precursor protein) and mostly consist of 40 ($A\beta_{1-40}$) and 42 ($A\beta_{1-42}$) residues. In a water environment, they are intrinsically disordered in the monomeric state but under specific conditions can aggregate into amyloid fibrils with a characteristic cross β-sheet structure.[9−12] Recent studies indicate that mature fibrils as well as soluble oligomers are the toxic agents inducing the cell death by various pathways.[6,13−17]

Amyloid aggregation of poly/peptides starts with unfolding or misfolding of native monomers, which results in conformational transition and loss of biological functions. Subsequently, misfolded monomers assemble into oligomeric nuclei acting as a core to recruit monomers to further grow into larger oligomers and presumably assemble into fibrils. A new understanding of fibril growth mechanism was provided by Jeong et al.[18] It was observed that fibrils fragmentized into small pieces can act as a new oligomeric nuclei to amplify aggregation. This new nuclei forming process is also known as "secondary nucleation" and has been identified in α-synuclein and Aβ peptide.[18,19] It was also reported that the "secondary nucleation" step is evitable if the concentration of protein is above a critical mass of fibril.[19]

Received: January 1, 2015
Revised: March 27, 2015
Published: March 27, 2015

ACS Publications © 2015 American Chemical Society

DOI: 10.1021/acs.jpcb.5b00006
J. Phys. Chem. B 2015, 119, 5145−5155

At present, no medication is available for AD, but there are evidence suggesting that reduction of amyloid assemblies can be favorable for animals and cells models of amyloidosis.[15,20−22] Morgan et al. have shown that laminin-1 can cause complete disassembly of fibrils into protofilaments and amorphous aggregates.[23] Fibril disaggregation induced by laminin-1 also contributed to the prevention of amyloid toxicity on hippocampal neuronal cells. Khlistunova et al.[15] observed that expression of the repeat domain of τ in N2a cell lines led to robust aggregation of τ and formation of Alzheimer-like paired helical filaments with high cytotoxicity. It was found that addition of the *N*-phenylamine inhibitors after formation of the fibrils in the cells caused that level of aggregation was reduced to 50% of the controls. Moreover, the toxicity caused by presence of tau aggregates was also decreased nearly to control levels. These findings indicate that prevention of protein self-assembly into amyloid structures or the clearance of amyloid deposits could be achievable strategy to treat amyloid-related diseases. A huge number of inhibitors for Aβ aggregation have been identified including carbohydrate-containing compounds,[24−29] polyamines,[30,31] chaperones,[32] metal chelators,[33] osmolytes,[34] RNA aptamers,[35] and other compounds.[36−39] Preclinical and clinical studies have shown that nutraceuticals might be valuable therapeutic agents for AD.[36,40−42]

Another strategy to affect Aβ aggregation is to use short peptides.[43,44] Since Aβ is self-assembling, fragments extracted from wild-type protein can serve as peptide-based inhibitors.[45−50] In particular, because the initial step of Aβ fibrillization strongly depends on residues 17 to 20 (LVFF) in the CHR (central hydrophobic region),[51] many studies have been focused on developing β-sheet breaker peptides to block this region. Tjernberg et al. showed that peptide KLVFF (fragment Aβ_{16-20}) shows significant binding to Aβ peptides preventing their self-assembly into fibrils.[45] Soto et al. have adopted a different design strategy directly focusing on the LVFFA (Aβ_{17-21}) motif, CHR of Aβ, and designed peptides with comparable hydrophobicity and sequences.[46,52]

Residues of Proline which had been previously recognized to reduce β-sheet propensity[53] were inserted in peptide-based inhibitors adding charged residues to the ends for enhancement of their solubility.[46,52] It has been shown that LVFFA has low ability to prevent Aβ fibrillization, but LPFFD, obtained by dual mutation V18P and A21D in this fragment, considerably improves it.[46,52] The impact of short fragments, extracted from C-terminal of Aβ peptide, on Aβ self-assembly was intensively studied by computer simulation.[48,50] The new structure-based peptide inhibitor design has been proposed using fibril-like crystal structures of short peptides with a "steric zipper" core as targets.[54] This allows one to develop non-natural peptide inhibitors.[55]

One of the most notable shortcomings of previously designed peptides containing at least 5 amino acids is that they are relatively long. Such big compounds may not satisfy the Lipinski's restriction[56] on mass. One can overcome this drawback using the shorter peptides, but Tjernberg et al. have suggested that for good binding the peptide should consist at least from five residues. This assumption was supported by experimental data which showed that tripeptides are weakly bound to Aβ peptides.[45,46] However, the experiments were performed for a small set of tripeptides, and it remains unclear if other tripeptides, especially those which contain rings, have better binding affinity or not.

Here we performed a systematic study of binding of all possible three amino acid peptides (8000 = 20^3 tripeptides in total) to Aβ fibrils using the docking method. Top-hits revealed by the virtual screening were further studied by a more precise MM-PBSA (molecular mechanics Poisson−Boltzmann surface area) method[57] which showed that WWW, WPW, WWP, and PWW have the highest binding affinity to Aβ fibrils. Depolymerizing activities of these tight binding tripeptides along with those determined by *in silico* screening as weak (IVL, VLA) or none (GAM, AAM) binders were tested experimentally *in vitro* using atomic force microscopy and fluorescence ThT assay. The obtained experimental data suggest the correlation between predicted binding affinities of tripeptides and their ability to depolymerize Aβ fibrils. In case of top lead tripeptides the DC_{50} values were determined in micromolar range, while only negligible depolymerizing activities were observed for the other tripeptides studied *in vitro*. Our data point out that the presence of specific aromatic as well as five-member rings is crucial for depolymerizing activity of tripeptides. We recommend top-hit tripeptides for further study as potential therapeutics for AD.

MATERIALS AND METHODS

Structure of Aβ_{9-40} Peptides. The sequence of Aβ_{1-40} iswhere hydrophobic residues are highlighted in blue. Because

$$\mathbf{DAEFR_5HDSGY_{10}\ EVHHQ_{15}KLVFF_{20}AED\ VG_{25}SNKGA_{30}IIG\ LM_{35}\ VGGVV_{40}}$$

the first 8 amino acids of Aβ_{1-40}[58] are unstructured, we consider fibrils of truncated peptides 6Aβ_{9-40}. Their atomic structure, resolved by solid state NMR, was taken from PDB (protein data bank) with entity 2LMN.pdb but keeping only one layer[58] to reduce the computational cost. It should be noted that 6Aβ_{9-40} which is among smallest protofibrils but yet stable structures. The rationale of our choice is also supported by the well documented fact that oligomeric species are cytotoxic[16] although the abundance of Aβ_{40} hexamers remains largely unknown.[59,60]

Parameters of Ligands. From 20 amino acids, one can construct 8000 tripeptides. For simulations their structures have been generated by using AMBER 11 package.[61] To avoid possible bad contacts arising from close atoms, all structures were minimized using implicit water model and the GB (Generalized Born) approximation.[62] The cutoff 99 Å was used for nonbond interactions. The maximum number of cycles of minimization was 1000, in which the steepest decent method was applied for the first 500 cycles and then switching to other last circles by the conjugate gradient method. The optimized structures were used for further docking simulations.

Docking Method. To dock tripeptides to Aβ fibrils, the PDBQT file for receptors and ligands was prepared by AutodockTools 1.5.4.[63] Autodock Vina version 1.1[64] has been employed for estimation of binding energies. In this software, for local structure optimization the Broyden−Fletcher−Goldfarb−Shanno method[65] is used. For global search, we set the exhaustiveness equal 300, and the maximum difference between energies of the best and the worse binding modes as large as 7 kcal/mol. Twenty binding modes were generated starting from random configurations of fully flexible ligand, keeping the receptor rigid. To cover the entire 6Aβ_{9-40}, we have chosen grid box of 80 × 50 × 65 Å^3. The receptor center of mass was positioned at the same place as the grids center.

DOI: 10.1021/acs.jpcb.5b00006
J. Phys. Chem. B 2015, 119, 5145−5155

Molecular Dynamic Simulation. To go beyond the inaccurate docking method, the binding affinity of the ten top-hit compounds, revealed by docking, was also estimated by MD (molecular dynamics) simulation using all-atom modeling with explicit water. 6Aβ_{9-40}-tripeptide complexes were solvated in a cubic box of around 19500 water molecules keeping the distance between the box surface and solute as large as 1 nm. In order to minimize size effects the periodic boundary conditions were imposed. The 1.0 and 1.4 nm cutoff were adopted for electrostatic and vdW interactions, respectively. The long-range Coulomb electrostatic interaction was calculated by the particle-mesh Ewald (PME) method.[66] The Langevin equation for motion was solved by the leapfrog algorithm.[67]

First, the system was minimized to avoid local strains in the protofibril and bad contacts with aqueous environment. A minimization procedure was performed using the conjugate gradient and steepest descent methods. This step was converged once the maximum force drops below 20 fN. Keeping atoms of 6Aβ_{9-40} restrained evenly distributed systems were obtained by relaxation for 100 ps. After gradual heating to 300 K, the equilibration was obtained in the heat bath. Using Berendsen algorithm[68] and a damping coefficient 0.1 ps the constant T = 300 K was achieved during NVT simulation of 50 ps. For NPT simulation at 1 atm we employed the Parrinello−Rahman method[69] and the damping coefficient of 0.5 ps. MD simulations were performed using force field AMBER99SB[70] and model TIP3P[71] for water molecules. They are implemented in the Gromacs-4.5 package.[72] Note that the combination of force field AMBER99SB and TIP3P is the best one for studying the binding of small molecules to proteins[73]

MM-PBSA Method. The MM-PBSA method[57] was applied to refine the binding affinity of top leads obtained by the docking method. Its details are given somewhere[74−76] (see also Supporting Information). The ligand binding free energy to receptor is defined by the following equation:

$$\Delta G_{\text{bind}} = \Delta E_{\text{vdw}} + \Delta E_{\text{elec}} + \Delta G_{\text{PB}} + \Delta G_{\text{sur}} + -T\Delta S \quad (1)$$

where ΔE_{vdw} and ΔE_{elec} are vdW and coulombic interactions. ΔG_{PB} and ΔG_{sur} represent polar and nonpolar solvation energies, respectively. The entropic term $T\Delta S$ was computed in the normal mode approximation.[77] In order to obtain ΔG_{bind}, the 20 ns MD trajectories were generated with starting protofibril−tripeptide configurations obtained in the lowest-energy docking modes. Then ΔG_{bind} was estimated using eq 1 and collected in equilibrium snapshots.

Contact Maps. A simple way to visualize 6Aβ_{9-40}-tripeptide interactions is to use the SC-SC (side chain-side chain) contact map. A SC-SC contact is counted when the distance between two side-chain centers of mass is less than 6.5 Å.

Chemicals. Aβ peptide Aβ_{1-40} (Cat. no. A-1001−2, Lot no. 10290940 T) was obtained from rPeptide (USA). Thioflavin T (ThT), NaOH, 3-(N-morpholino)propanesulfonic acid (MOPS), DMSO and NaN_3 have been purchased from Sigma-Aldrich and have been of analytical grade. Studied tripeptides H-Pro-Trp-Trp-OH (PWW), number 130104; H-Trp-Pro-Trp-OH (WPW) number 130105; H-Trp-Trp-Pro-OH (WWP) number 130106, H-Trp-Trp-Trp-OH (WWW), number 130103, H-Gly-Ala-Met-OH (GAM), number 130701; H-Ala-Ala-Met-OH (AAM), number 130702; H-Ile-Val-Leu-OH (IVL), number 130703, and H-Val-Leu-Ala-OH (VLA), number 130704 were purchased from the company VIDIA (Czech Republic). Samples were prepared by dissolving tripeptide in DMSO and subsequent dilution of 50 mM stock tripeptide solution just before the measurements, and the content of DMSO in samples was below 2% (v/v).

Aβ_{1-40} Amyloid Fibrillization. Lyophilized Aβ_{1-40} was dissolved in 10 mM NaOH to the 665 μM concentration. The peptide concentration was determined by UV−vis spectroscopy (JASCO V-630) using extinction coefficient of ϵ_{292} = 2300 M^{-1} cm^{-1}. The solution was sonicated in a bath sonicator for 1 min, then 10 min centrifuged (12 000 g) at 4 °C to precipitate the bigger aggregates. After the centrifugation, the concentration was measured again. The stock solution of Aβ_{1-40} has been diluted to final (10 μM) concentration in 150 mM 3-(*N*-morpholino)propanesulfonic acid (MOPS), 7 days incubated at 37 °C and pH 6.9. The presence of fibrils was confirmed by AFM (atomic force microscopy) and Thioflavin T (ThT) fluorescence assay.

ThT Fluorescence Assay. Amyloid fibrillization of the Aβ_{1-40} peptides was detected by a characteristic increase in ThT fluorescence intensity reflecting the occurrence of Aβ fibrils. ThT was added to samples containing 10 μM Aβ_{1-40} solution to a final concentration 20 μM and incubated for 1 h at 37 °C. The fluorescence intensity of ThT was measured using a 96-well plate by a Synergy MX spectrofluorimeter (BioTek). The excitation wavelength was chosen at 440 nm, while the emission spectrum was recorded at wavelength of 485 nm. The top probe vertical offset was 6 nm and the excitation and emission slits were adjusted to 9.0/9.0 nm.

Atomic Force Microscopy. Samples were deposited by drop casting on the freshly cleaved mica surface. After 5 min adsorption, the samples of peptide concentration 10 μM and tripeptides of 60 μM were left to dry after washing with ultrapure water. AFM images were obtained using a uncoated silicon cantilevers TESPA, unmounted with force constant 42 N/m and nominal resonance frequency 320 kHz, Al Reflective Coating (Bruker AFM Probes, Camarillo, USA) with Scanning Probe Microscope (Veeco di Innova, Bruker AXS Inc., Madison, WI) working in a tapping mode. The resolution of image was 512 pixels per line (512 × 512 pixels/image) and the scan rate was 0.25−0.7 kHz. No smoothing or noise reduction was applied.

Screening of Tripeptide Activity to Disassemble Aβ Amyloid Fibrils. The ability of tripeptides to degrade preformed Aβ_{1-40} fibrils was investigated using ThT assay. Tripeptides were dissolved in DMSO at 50 mM concentration; the content of DMSO in measured samples was below 2% (v/v) and had no impact on the Aβ_{1-40} fibril stability. The three different concentrations of tripeptides WWW, WPW, PWW, WWP, AAM, GAM, IVL, and VLA at final concentration of 1 nM, 60 μM and 1 mM, were added to the solution of 10 μM Aβ_{1-40} amyloid fibrils (150 mM MOPS buffer, pH 6.9) and incubated 24 h at 37° C. After incubation ThT was added to a final (20 μM) concentration and fluorescence intensity was recorded at the excitation wavelength of 440 nm and the emission wavelength of 485 nm. The fluorescence of tripeptides dissolved in 150 mM MOPS buffer was measured as a control. In our experiment each presented value is the average of the three independent measured values.

Determination of DC_{50}. DC_{50}, defined as concentration of tripeptide causing 50% reduction of the amount of Aβ_{1-40} amyloid fibrillar aggregates (10 μM), was measured by ThT assay.

Aβ_{1-40} fibrils (10 μM) in 150 mM MOPS were incubated 24 h (37 °C) with tripeptide at different concentrations ranged

DOI: 10.1021/acs.jpcb.5b00006
J. Phys. Chem. B 2015, 119, 5145−5155

from 100 pM to 1 mM. The fluorescence intensities of samples with tripeptides were normalized to the fluorescence signal of amyloid aggregates alone. Each presented value is the average of the three independent measured values. The DC_{50} values were defined from dose−response curves obtained by fitting the average values by nonlinear least-squares method. To fit experimental data we used sigmoidal equation (logistic), $y = (a/(1 + (x/x_0)^b))$, with three parameters a, b, and x_0.

RESULTS AND DISCUSSION

***In silico* Results.** *Ligands Preferably Bind to Hydrophobic Regions of 6Aβ_{9-40}.* At first, the binding poses for representative ligands were studied in detail. The first 20 best docking poses of each ligand fall in the one spot as it is evident from Figure S1 in the Supporting Information. Therefore, the lowest energy or best docking mode can be confidently accepted for further consideration. The binding energy ΔE_{bind} of tripeptides to 6Aβ_{9-40}, obtained in the best docking conformation, varies between −4.7 and −11.5 kcal/mol (Figure S2 in Supporting Information). About 30% ligands have $\Delta E_{bind} \approx -7$ kcal/mol. Figure 1 shows binding positions of all ligands

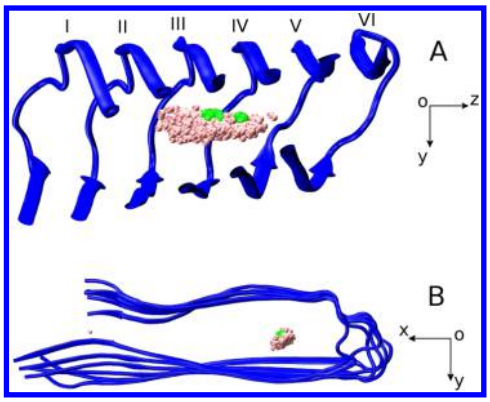

Figure 1. Binding positions of the tripeptides to 6Aβ_{9-40} with view perpendicular (A) and along the fibril axis z (B). The chains of receptor (blue) are numbered as I, II, III, IV, V and VI. Small pink spheres refer to tripeptides while the representative top-hit binders shown in Table 1 are highlighted by larger green spheres. Each tripeptide is represented by a sphere positioned at its center of mass. Results were obtained in the best binding mode.

to 6Aβ_{9-40}. A lot of compounds are located near the loop region inside fibril because this region is wider compared to other regions. The top leads are also found in this region. Only a few compounds are positioned near terminals of peptides. A detailed SC-SC contact map analysis shows that ligands mainly interact with residues 19, 21, 30, and 32 of II−V peptides of 6Aβ_{9-40} (Figure S3 in Supporting Information). Because 19, 21, 30, and 32 are hydrophobic residues (see Materials and Methods) one can conclude that ligands predominantly bind to hydrophobic regions. This is consistent with the scanning experiment of Tjernberg et al.[45] who have shown that short peptides extracted from Aβ_{1-40} bind to its hydrophobic regions better than other regions. Moreover, in agreement with the MM-PBSA results that the electrostatic contribution is important (see below), the charged residue 23 of IV−V, and 28 of II−III peptides also strongly interact with ligands (Figure S3 in Supporting Information).

Proline Enhances Binding Affinity. One can show that binding affinity of tripeptides increases with a number of parameters such as mass, number of carbon atoms, number of aromatic residues, van der Waals volume of side chains, and molar refractivity of ligands. Since this conclusion was also previously obtained for nonpeptide ligands,[78−82] we focus on the role of proline.

Proline is unique among 20 natural amino acids because its side chain cyclic structure locks the backbone ϕ dihedral angle at approximately -75^o, making its conformation exceptionally rigid compared to other amino acids. As a result, proline rarely appears at the center of α-helix and β-sheet structure.[83,84] It can disrupt β-sheet in both aqueous and membrane environments.[85] Insertion of proline residue in β-sheet breaker peptides increases their ability to slow down the fibril formation.[46,75] From this point of view, proline deserves particular attention among other amino acids.

To clearly demonstrate the influence of proline, the difference between average binding energies of tripeptides with and without Proline is plotted against the number of HA (heavy atoms) (Figure 2). Here $\overline{\Delta E}_{bind}$ for ligands with proline

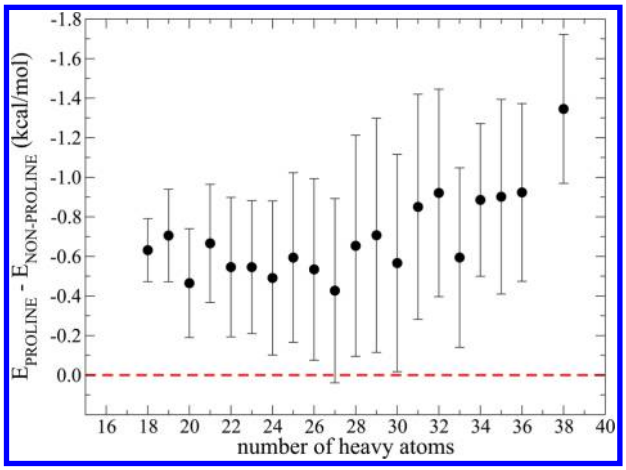

Figure 2. Binding energy difference between ligands with and without proline residue. Results were obtained by averaging over all ligands that have the same number of HA.

is calculated in such a way that for a given number of HA we average over all tripeptides containing at least one proline. Proline always enhances the binding and for $N_{HA} = 38$, ΔE_{bind} is reduced by ≈1.4 kcal/mol, leading to decrease of DC_{50} by 1 order of magnitude. More accurate methods for estimation of binding affinity may give a stronger effect. Thus, due to conformational rigidity, Proline reduces the entropy cost leading to binding enhancement. This relevant factor should be taken into account at least for drug design for diseases associated with protein aggregation.

To compare proline with other residues the dependence of $\overline{\Delta E}_{bind}$ on amino acids was considered (Figure S4 in Supporting Information). Proline (P) and histidine (H) are presumably comparable in binding affinity probably because both of them have one 5-membered ring. Phenylalanine (F), tyrosine (Y), and tryptophan (W) are better than proline as they all have an aromatic ring. This is in accord with previous works about the importance of aromatic rings in inhibition of the amyloid aggregation[74,86−88] and our docking results showing that ΔE_{bind} increases with the number of aromatic residues and rings (Figure S5 in Supporting Information). Since ΔE_{bind} also correlates with the number of atoms and mass of tripeptides (Figure S5 in Supporting Information), the better

DOI: 10.1021/acs.jpcb.5b00006
J. Phys. Chem. B 2015, 119, 5145−5155

Table 1. Binding Energies of PWW and the Top Ten Tripeptides Revealed by the Docking Method.[a]

Ligand	ΔE_{vdW}	ΔG_{sur}	ΔE_{elec}	ΔG_{pb}	$-T\Delta S$	ΔG_{bind}	E_{dock}
WWW	-64.57	-8.95	-99.37	138.51	25.03	-9.34 ± 2.04	-11.5
WWP	-51.08	-7.02	-88.64	113.81	19.78	-13.15 ± 2.25	-11.2
WWY	-39.88	-6.64	-62.88	77.67	23.11	-8.64 ± 1.83	-11.0
WWF	-53.55	-8.18	-104.87	138.58	22.73	-5.27 ± 2.12	-10.9
YWW	-61.61	-7.03	-94.87	129.97	25.62	-7.94 ± 1.92	-10.9
WPW	-48.63	-7.80	-65.53	90.31	20.33	-11.32 ± 1.85	-10.8
FWW	-51.70	-8.03	-84.99	114.71	23.20	-6.81 ± 2.78	-10.8
WFW	-52.54	-8.62	-82.70	112.91	23.65	-7.29 ± 2.11	-10.7
WYW	-42.42	-6.07	-60.10	77.96	23.61	-7.02 ± 1.77	-10.7
WFP	-50.03	-7.17	-29.88	59.75	19.82	-7.52 ± 1.45	-10.6
PWW	-49.50	-7.94	-94.40	120.34	20.42	-11.08 ± 2.17	-10.4

[a]Binding free energies obtained by the MM-PBSA method are also shown. Energies are in kcal/mol.

binding of phenylalanine, tyrosine, and tryptophan compared to proline may be due to their larger size and weight.

Tryptophan is the best one with one 5-membered ring more. Glycine (G) which does not have a side chain is ranked last. Cysteine also contributes little to binding with amyloid fibril. It should be note that this interpretation is just based on the docking results and may be oversimplified because these residues are also different in other ways. The departure from general trends mentioned here should be studied carefully using more precise methods and MD simulations.

Prediction of Top-Leads by Docking and MM-PBSA Simulations. Docking Results. From 8000 peptides we have selected the 10 top hits which have the lowest binding energy to receptor 6Aβ_{9-40} (Table 1). These compounds are composed mostly of W, P, F, and Y that have aromatic and 5-membered rings. WWW is a champion probably because it has the largest number of rings. Proline occurs in the three top compounds, and this is in line with the fact that Proline greatly enhances the binding to 6Aβ_{9-40} (Figure 2).

For comparison with the top hits, among middle binders we select IVL (ΔE_{bind} = −7.5 kcal/mol) and VLA (ΔE_{bind} = −7.2 kcal/mol) while among weak binders AAM (ΔE_{bind} = −5.6 kcal/mol) and GAM (ΔE_{bind} = −5.4 kcal/mol) are chosen for further *in vitro* study (see below).

Having used the docking method we obtained ΔE_{bind}= −8.8 and −9.5 kcal/mol for LVFFA and LPFFD, respectively. This is consistent with the experiments of Soto et al.[46,52] that LPFFD displays the higher inhibition capacity than LVFFA due to the presence of proline. As follows from Table 1, the binding energies of top-hits, obtained by the docking method, vary between −10.4 and −11.5 kcal/mol. Thus, the absolute values of ΔE_{bind} of LVFFA and LPFFD are lower and they are expected to bind to Aβ weaker than top-hits.

Tjernberg et al.[45,89] have performed *in vitro* study for 10 tripeptides listed in Table S2 in Supporting Information. Among them only three peptides VFF, FFA, and LVF showed very low activity. This result is consistent with our docking simulations because these peptides have the absolute values of ΔE_{bind} larger than the remaining seven tripepeptides which had no activity at all. On the basis of the docking results, one can also expect that VFF, FFA, and LVF have lower binding affinity compared to top-leads shown in Table 1.

Usually the docking method is useful in locating binding sites but its predictive power for binding affinity is limited because the dynamics of receptor is ignored and the number of position trials for ligand is finite. Therefore, in further calculations the more accurate MM-PBSA method was used to refine docking predictions.

Ranking by MM-PBSA. Because the simulations by MM-PBSA methods are CPU time-consuming we restrict our study to 10 top leads shown in Table 1. Note that WPW and WWP are among the top leads but not PWW. However, we will also consider PWW not only because of its binding energy close to top-hits but also because of the important role of proline as β-sheet breaker. Configurations, obtained in the best docking mode, were used as starting structures for MD runs. During 20 ns MD simulations ligands stay inside the target (see Movie 1 in the Supporting Information). All-atom RMSD (root-mean-square displacement) of the receptor relative to its initial structure is plotted against time (Figure 3) for 10 tripeptides.

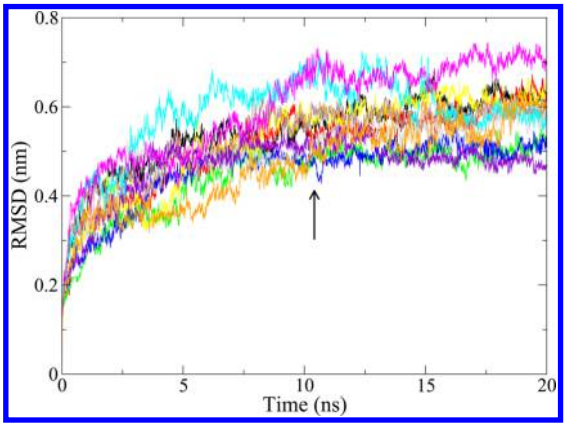

Figure 3. Time dependence of the all-atom RMSD of 6Aβ_{9-40} in the presence of different tripeptides. Black, red, green, blue, yellow, brown, gray, violet, cyan, magenta and orange, respectively, refer to WWW, WWP, WWY, WWF, YWW, WPW, FWW, WFW, WYW, WFP, and PWW. The arrow refers to the time when systems reach equilibrium.

Overall, the systems reach equilibrium after 12 ns when the RMSD curve gets saturation. ΔG_{bind} was computed using the MM-PBSA method and snapshots collected in the last 8 ns. The results are shown in Table 1.

Except WFP the Coulomb interaction is superior to the vdW interaction. An interesting question emerges: why WFP is so different from other tripeptides in term of ΔE_{elec}? To address this question we consider WFP and three representative tripeptides WWW, PWW and WWP in more detail. The atomic indices and charges of these peptides is given in Table S1 in the Supporting Information. Because of polarization effect in water, the N-end and C-end have positive and negative charges (Table S1 in Supporting Information), the first and third residues of tripeptides prefer to bind to the region containing charge residues GLU22, ASP23 and LYS28 (Figures S6−S9 in

DOI: 10.1021/acs.jpcb.5b00006
J. Phys. Chem. B 2015, 119, 5145−5155

Supporting Information). They also interact with hydrophobic residues PHE19, ALA21, ALA30, ILE31, ILE32 and LEU34 locating closely the salt-bridge region. The first and third residues prefer to locate next to the negatively charged ASP23 and positively charged LYS28, respectively (Figures S6−S9 in the Supporting Information).

The electrostatic interaction of WWW and WWP with fibril dominates over WFP because they often form contact with ASP23 and LYS28 (Figures S6 and S7 in the Supporting Information), while WFP mostly interacts with LYs28 (Figure S8 in the Supporting Information). On the basis of the contact maps presented in Figures S8 and S9, it is not clear why the electrostatic interaction of WFP is weaker than PWW because both of them mainly interact with LYS28. To shed light on this problem we present contributions from individual atoms of tripeptides to the Coulomb part (Figure S10 in the Supporting Information). The domination of PWW over WFP comes from difference in contribution of the last atoms C, OC1 and OC2 as well as atom HE1 at position 28 of PWW.

Comparing WFP with WWW and WWP (Figure S10 in Supporting Information) one can see that the contribution of the first residue W was significantly reduced due to the presence of amino acid F. The mutation W by F weakens the electrostatic interaction of the last residue P with the receptor if one compares WWP with WFP. Thus, the poor electrostatic interaction of WFP may be understood studying its per-atom distributions.

For all four tripeptides the two last atoms OC1 and OC2 have strong attractive interaction with the fibril, while their neighbor atom C experiences the repulsion. This is because negatively charged CO1 and OC2 and positively charged C atom (Table S1 in Supporting Information) interact with LYS28 carrying positive charge. The importance of rings in electrostatic interaction is evident for WWW, WWP, and PWW (Figure S10 in Supporting Information).

The contribution of electrostatic interaction is over compensated by polar solvation energies, resulting to all positive numbers. The level of positive sums $\Delta E_{elec} + \Delta G_{GP}$ (from 15 to 40 kcal/mol) also orients the ranking by MM-PBSA. Thus, the negative values of ΔG_{bind} come from vdW energies which vary from −62 to −40 kcal/mol. This observation once again proves that hydrophobicity alone does not control binding propensity, but it is indispensable to direct the reaction. Apolar solvation energies constitute to the final binding scores at the same range (from −9 to −6 kcal/mol) in all compounds (Table 1), while ΔG_{PB} greatly varies across the whole set of ligands. The entropy changes upon binding are quite different among various structures, from 19.8 to 25 kcal/mol. A peptide which has complex rings that lie close may have low entropy. The deviation in entropy partially affects the final binding propensity. Three compounds containing Proline have the lowest entropic contribution because as mentioned above the conformation of this residue is highly rigid. Specifically, WWP which has the least positive entropy value has the highest potential to degrade the Aβ amyloid fibrils. As follows from Table 1 ΔG_{bind} is sensitive to sequences of ligand amino acids. WPW is a bit worse than WWP because when Proline is in the middle the complex becomes energetically less favorable due to decrease of both vdW and Coulomb interaction. Within the error bars, the binding free energies of WPW, WWP, and PWW are comparable. The binding strength to 6Aβ_{9-40} has been optimized when F is inserted between two W amino acids but it becomes worse in the case of Y because WYW has the binding affinity lower than YWW and WWY.

One can understand difference in binding affinity of tripeptides at the atomistic level considering the per-atom distributions of the interaction energy involving the electrostatic and vdW terms (Figure S11). In WWW atoms 14 (HE1), 38 (HE1), 61 (NE1), 62 (HE1), 73 (C), 74 (OC1), and 75 (OC2) play the most important role. The contribution of atoms from residues W of tripeptide WWP is almost the same as the first two residues W from WWW. For WWP, in addition to atoms at position 14 (HE1) and 38 (HE1), atoms 63 (C), 64 (OC1), and 65 (OC2) are prominent in binding (Figure S11). Comparison of PWW with WWP reveals the importance of position of P in per-atom distributions of interaction energies. Together with atom 28 (HE1) atoms 63 (C), 64 (OC1), and 65 (OC2) contribute to the binding affinity of PWW to greater extent than for WWP. Despite great variations in per-atom distributions the total binding free energy of WWW, WWP, and PWW remains almost the same (Table 1). The WFP case (Figure S11 in Supporting Information) is different because the overall behavior of the distribution is similar to WWP but the magnitude of interaction is reduced resulting in poor binding. Atoms O at position 26 and 46, and atoms 59 (C), 60 (OC1), and 61 (OC2) are important in this case.

As expected, the ranking of top leads obtained by the docking method is altered by the MM-PBSA simulations. WWP, second by docking ranking, becomes champion in the MM-PBSA classification having the lowest $\Delta G_{bind} = -13.15$ kcal/mol (Table 1). WWW, which is the first among docking top hits, is ranked third now. We predict that WWP, WPW, PWW, and WWW are the most prominent binders to Aβ fibrils having $\Delta G_{bind} < -9$ kcal/mol. The binding constant DC_{50} might be estimated by the formula $DC_{50} = K_I = \exp(\Delta G_{bind}/RT)$, where R is gas constant and unit of K_I is mol. Using ΔG_{bind} from Table 1 one obtains the binding constant $DC_{50} \approx$ 160, 3.5, 21.9, and 27.8 nM for WWW, WWP, WPW and PWW, respectively. Thus, DC_{50} of the four top hits falls in the submicromolar range. Experimentally, Tjernberg et al.[45,89] have found that tripeptides extracted from full-length Aβ peptides have very low binding affinity to Aβ fibrils. This is because their peptides do not contain proline. Our simulations show that proline and residues with rings can enhance the binding of tripeptides to Aβ.

***In vitro* Investigation of the Ability of Tripeptides To Depolymerize the Aβ_{1-40} Fibrils and Determination of DC_{50} Values.** *Screening of Depolymerizing Activities of Tripeptides.* The ability of tripeptides to depolymerize Aβ fibrils was investigated experimentally by ThT fluorescence assay. The interaction between ThT and Aβ fibrils leads to significant increasing of fluorescence intensity of ThT (Figure 4, violet line) that is not observed for the native Aβ peptide (Figure 4, violet dotted line). The fluorescence intensities detected after incubation of Aβ fibrils with studied tripeptides (200 μM) are presented in Figure 4. The abilities of tripeptides to depolymerize Aβ fibrils negatively correlate with fluorescence intensities; namely, the lower fluorescence values correspond to the greater depolymerization activities. Data indicate different effect of tripeptides on amyloid fibrils. Intensive decrease of ThT fluorescence intensities was obtained for samples of Aβ fibrils incubated with tripeptides selected by *in silico* experiment as the best binders. For tripeptides predicted to be very weak binders (GAM and AAM), the fluorescence intensities are comparable to that observed for Aβ

DOI: 10.1021/acs.jpcb.5b00006
J. Phys. Chem. B 2015, 119, 5145−5155

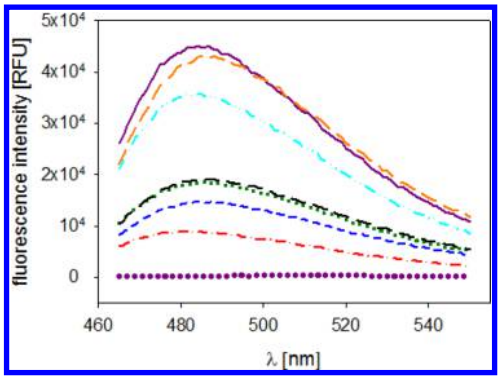

Figure 4. ThT fluorescence spectra of native Aβ_{1-40} 10 μM; violet dots) and Aβ_{1-40} fibrils (10 μM) in the absence (solid violet line) or in the presence of 200 μM of tripeptides WWW (black long dash line), WWP (blue short dash line), WPW (dark green dotted line), PWW (red dash−dot line), GAM (orange dash line), and IVL (cyan dash dot−dot line).

fibrils alone (data shown only for GAM). In case of tripeptides for which middle binding affinities were predicted by the docking method (IVL and VLA) only moderate decline of fluorescence was detected (data shown only for IVL).

The destroying activities were further investigated for three different tripeptide concentrations (1 nM, 60 μM, and 1 mM); fluorescence intensities which were normalized to the intensity of untreated fibrils are presented in Figure 5. It was found that

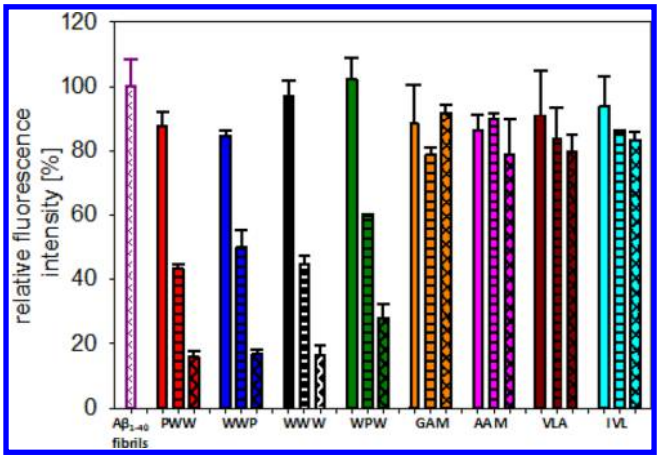

Figure 5. Fluorescence intensities for Aβ_{1-40} fibrils (10 μM) alone and after incubation with tripeptides at concentration of 1 nM (solid bars), 60 μM (bars with lines), and 1 mM (bars with crossing lines) detected by ThT assay. Fluorescence intensities were normalized to the fluorescence of signal of untreated Aβ fibrils.

ability of tripeptides selected as top-leads (WWW, PWW, WPW, and WWP) to depolymerize Aβ fibrils is concentration dependent. For highest tripeptide concentration (1 mM) the significant decrease of fluorescence intensities compare to fluorescence of Aβ fibrils alone was detected. The highest disassembly activities corresponding to the lowest fluorescence intensities were observed for tripeptide PWW, WWP, and WWW (A_{dep} 83%). Only slightly smaller depolymerization was observed for WPW (A_{dep} 72%). Tripeptides GAM and AAM characteristic of very low affinity to bind to Aβ fibrils display no significant decline of fluorescence even at higher concentrations, ThT fluorescence intensities are comparable to that observed for Aβ fibrils alone (Figure 5). These data suggest almost no depolymerizing activities of these tripeptides (A_{dep} ~ 5−10%). Very slight decrease of fluorescence was detected for the highest concentrations of tripeptides with weaker binding affinities (VLA and IVL) corresponding depolymerizing activity A_{dep} of about ~10−15%.

AFM. The influence of tripeptides on the Aβ fibril patterns was also investigated by AFM to directly visualize their disassembly abilities. Representative AFM images are presented in Figure 6. The incubation of tightly binding tripeptides WWW, PWW, WPW, and WWP with Aβ fibrils led to extensive reduction of the overall amount of the fibrillar self-assemblies compare to untreated Aβ fibrils (Figure 6B−E). In dependence on the tripeptide composition the different changes in shape and size of aggregates were observed. For tripeptide containing only Tryptophanes (WWW) the fibrils are much shorter compare to Aβ fibrils. Presence of PWW and WPW caused disassembly of fibrils to very short structures with tendency to accumulate into clusters mainly in case of PWW. Interestingly, incubation of Aβ fibrils with WWP led mostly to formation of globular structures. AFM images clearly demonstrate that tripeptides selected as top-leads have significant ability to depolymerize Aβ fibrils, and hence support the experimental data obtained by ThT assay as well as results from docking calculations.

The interactions of Aβ fibrils with weaker binders (IVL, VLA) and tripeptides with very low binding affinity to fibrils (GAM, AAM) were observed by AFM as well. Representative AFM images obtained for GAM and IVL (Figure 6F,G) show that presence of these tripeptides caused no significant changes; the fibrils have similar morphology to that detected for Aβ fibrils. Thus, obtained AFM images support minimal or neither evidence of fibril depolymerization for these tripeptides determined by ThT assay. It should be mentioned that all studied tripeptides do not form any fibrillar or amorphous structures at conditions used for examination of depolymerizing abilities, the representative image obtained for tripeptide WWP is presented in Figure 6H.

Determination of DC_{50}. ThT assay was employed to obtain the DC_{50} values for all experimentally studied tripeptides. The depolymerizing activities of studied tripeptides in concentration region from 10 pM to 1 mM were tested at Aβ_{1-40} fibril concentration of 10 μM. The normalized fluorescence intensities (to the signal of amyloid fibrils alone) obtained for tightly binding tripeptides WWW, PWW, WPW, and WWP are present in Figure 7A. Using dose-dependent curves, which were obtained by fitting of fluorescence intensities, the DC_{50} values of half-maximal disassembly were determined (Table 2). DC_{50} is in μM range, and the lowest DC_{50} value was obtained for PWW (1.6 μM), while a slightly higher DC_{50} values were found for remaining tight binding tripeptides, namely 47.1 ± 4.1, 55.8 ± 1.6, and 73.9 ± 2.2 μM for WWP, WWW, and WPW, respectively. Since a change in ΔG_{bind} by 1 kcal/mol results in change of binding constant by about 1 order of magnitude, DC_{50}, obtained by experiment for PWW, is still consistent with our MM-PBSA results within the error bars (Table 1).

The concentration dependencies of depolymerizing abilities were examined also for tripeptides characteristic of weaker (IVL, VLA) and very low (GAM, AAM) binding affinity to fibrils. The observed fluorescence intensities for GAM and VLA tripeptides presented in Figure 7B clearly indicate no disassembly of fibrils. The similar results were observed for AAM and IVL tripeptides.

DOI: 10.1021/acs.jpcb.5b00006
J. Phys. Chem. B 2015, 119, 5145−5155

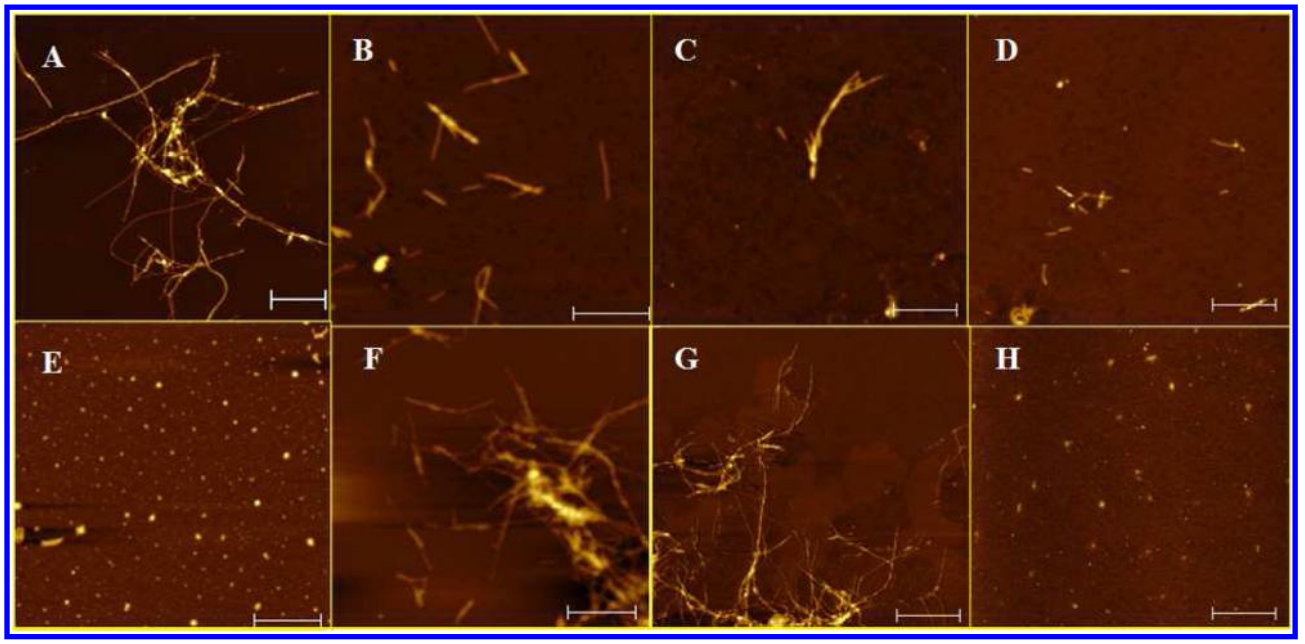

Figure 6. AFM images of Aβ_{1-40} fibrils (10 μM) (A) and after their incubation with 60 μM of tripeptide (B) WWW, (C) PWW, (D) WPW, (E) WWP, (F) GAM, and (G) IVL. (H) Representative AFM image of WWP tripeptide alone. The similar AFM images were observed for other alone tripeptides. Bars represent 1 μm.

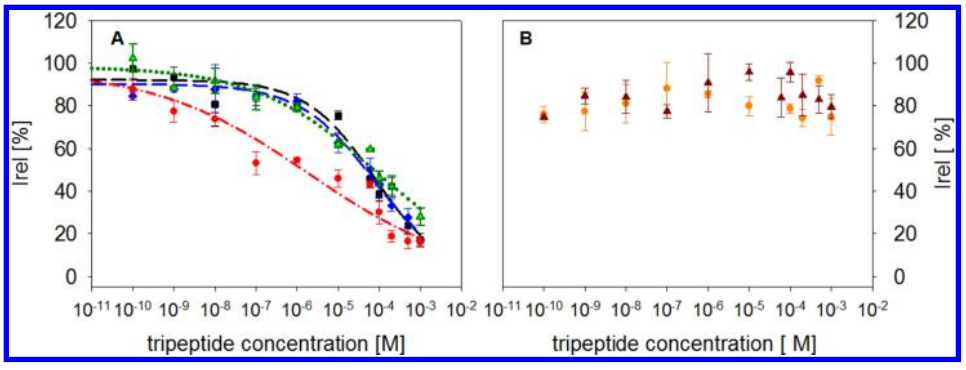

Figure 7. Determination of DC_{50} values of tripeptides by ThT assay: (A) PWW (red circles), WPW (green triangles), WWP (blue diamonds), and WWW (black squares); (B) GAM (orange circles) and VLA (brown triangles). The effect of increasing tripeptide concentrations on A fibrils was quantified by normalizing fluorescence intensity to the control (100% fluorescence intensity of the Aβ fibrils in the absence of tripeptide). A single experiment was performed with each sample in triplicates. The error bars represent the average deviation for repeated measurements of three separate samples. The curves were obtained by fitting of the average values by a nonlinear least-squares method.

Table 2. Experimentally Determined Values of DC_{50} for Studied Tripeptides[a]

DC_{50} (μM)					
WWW	PWW	WPW	WWP	GAM, AMM	IVL, VLA
55.8 ± 1.6	1.6 ± 0.4	73.9 ± 2.2	47.1 ± 4.1	N/A[b]	N/A[b]

[a]Results were obtained for 10μM concentration of Aβ_{1-40} fibrils. [b]N/A - not available due to no or very low depolymerizing activity.

Relationship between Tripeptide Composition and Depolymerizing Activity. The data obtained by simulations and *in vitro* experiments demonstrate influence of tripeptide composition on both the binding affinities to Aβ fibrils and depolymerization activities. The both approaches clearly indicate that presence of cyclic amino acid proline and aromatic amino acid tryptophan in tripeptides is crucial for their tight binding to Aβ fibrils as well as for significant depolymerizing ability. We assume that multiple occurrences of amino acid heterocycles increase the capacity of these tripeptides to interact with amyloid fibrils. The adjacent localization of tryptophans possessing a couple of rings can significantly improve the interaction of these cycles with β-sheets stabilizing amyloid fibrils. The importance of the presence of aromatic residues was also shown by Azriel and Gazit et al.[90] Their results clearly indicate that a doubled aromatic phenylalanine residue ("FF" motif) is a major structural motif mediating interactions of short peptides QKLVFF, LVFFA, and LPFFD with Aβ. In the case of proline, it was shown that insertions of this residue to the β-sheet breaker peptides slow down the Aβ fibrillization.[75] We assume that extensive depolymerizing activities of our tightly bind tripeptides are due to presence of complex heterocycle structure possessing interactions which are able to block π-stacking interactions of fibrils. The proposed assumption of tight binding tripeptides to depolymerize Aβ fibrils is supported by results observed for tripeptides consisting of hydrophobic but noncyclic residues. The absence of cyclic

DOI: 10.1021/acs.jpcb.5b00006
J. Phys. Chem. B 2015, 119, 5145−5155

structures caused that interactions between the tripeptide and bonds forming the fibrils were not sufficient to destroy them.

CONCLUSIONS

The binding affinity of a set of 8000 tripeptides, all the possible combinations of amino acids in tripeptides, to 2-fold symmetry 6Aβ_{9-40} fibrils has been studied by the Autodock Vina method. One of the most interesting findings here is that, in agreement with the experiments,[45] tripeptides preferably locate near hydrophobic residues of receptor.

Together with other amino acids that contain rings the proline residues was present in most of top hit tripeptides as the rigidity of its 5-membered ring enhances the tripeptide binding affinity. More aromatic residues would give rise to stronger binding, but to satisfy Lipinski's rules[56] drug-like compounds cannot have many aromatic rings.

Top-hits revealed by the virtual screening were further studied by the more precise MM-PBSA method which shows that WWW, WPW, WWP, and PWW have the best ability to bind to Aβ fibrils (DC_{50} values ~ nM−μM). Depolymerizing activities of tight binding tripeptides along with weak or none binders were tested experimentally *in vitro* using AFM and ThT fluorescence assay. Our results suggest the significant correlation between predicted binding affinities of tripeptides and their ability to depolymerize Aβ fibrils.

We assume that presence of cyclic amino acid proline and aromatic amino acid tryptophan in tripeptides is crucial for their tight binding to Aβ fibrils as well as for significant depolymerizing ability. We suppose that multiple occurrences of amino acid heterocycles can significantly increase the ability of top-hit tripeptides to reduce or interrupt the β-sheets bonds stabilizing amyloid fibrils, i.e., reduce them. The proposed assumption of tight binding tripeptides to depolymerize Aβ fibrils is supported by results observed for tripeptides consisting of hydrophobic but noncyclic residues. The absence of cyclic structures caused that interactions between the tripeptide and bonds forming the fibrils were not sufficient to destroy them. The top leads highly recommended for further study as potential leads for AD.

ASSOCIATED CONTENT

Supporting Information

Details of MD simulation, the atom index of tripeptides, docking poses, contact maps, dependence of the binding energy on amino acid types and atom types of ligands, and a movie showing the movement of WWP during 20 ns MD simulation. This material is available free of charge via the Internet at http://pubs.acs.org.

AUTHOR INFORMATION

Corresponding Authors

*(Z.G.) E-mail: gazova@saske.sk.

*(M.S.L.) E-mail: masli@ifpan.edu.pl.

Author Contributions

‡(M.H.V., K.S.) Contributed equally to the work

Notes

The authors declare no competing financial interest.

ACKNOWLEDGMENTS

We were supported financially by the Department of Science and Technology at Ho Chi Minh City, Vietnam; Narodowe Centrum Nauki in Poland (Grant No 2011/01/B/NZ1/01622); Vietnam National Foundation for Science and Technology Development (NAFOSTED) under Grant Number 106-YS.02-2013.01; EU SF Grants 26220220005 and 26110230097; and VEGA Agency Grant 0181 and UPJS Grant VVGS-2013-98. We are very thankful to TASK in Gdansk (Poland) for providing computational resources.

REFERENCES

(1) Henderson, A. S., Jorm, A. F. *Dementia*; John Wiley & Sons Ltd: Chicester, U.K., 2002; Chapter 1.

(2) Greene, J. D. W.; Baddeley, A. D.; Hodges, J. R. Analysis of the Episodic Memory Deficit in Early Alzheimers Disease: Evidence from the Doors and People Test. *Neuropsychologia* **1996**, *34*, 537−551.

(3) Price, B. H.; Gurvit, H.; Weintraub, S.; Geula, C.; Leimkuhler, E.; Mesulam, M. Neuropsychological Patterns and Language Deficits in 20 Consecutive Cases of Autopsy-Confirmed Alzheimer's Disease. *Arch. Neuro.* **1993**, *50*, 931−937.

(4) Esteban-Santillan, C.; Praditsuwan, R.; Ueda, H.; Geldmacher, D. S. Clock Drawing Test in very Mild Alzheimer's Disease. *J. Am. Geriatr. Soc.* **1998**, *46*, 1266−1269.

(5) Alonso, A.; Zaidi, T.; Novak, M.; Grundke-Iqbal, I.; Iqbal, K. Hyperphosphorylation Induces Self-Assembly of Tau into Tangles of Paired Helical Filaments/Straight Filaments. *Proc. Natl. Acad. Sci. U.S.A.* **2001**, *98*, 6923−6928.

(6) Hardy, J.; Selkoe, D. J. Medicine—The Amyloid Hypothesis of Alzheimer's Disease: Progress and Problems on the Road to Therapeutics. *Science* **2002**, *297*, 353−356.

(7) Citron, M. Strategies for Disease Modification in Alzheimer's Disease. *Nat. Rev. Neurosci.* **2004**, *5*, 677−685.

(8) Aguzzi, A.; O'Connor, T. Protein Aggregation Diseases: Pathogenicity and Therapeutic Perspectives. *Nat. Rev. Drug Discovery* **2010**, *9*, 237−248.

(9) Eanes, E. D.; Glenner, G. G. X-ray Diffraction Studies on Amyloid Filaments. *J. Histochem. Cytochem.* **1968**, *16*, 673−677.

(10) Kirschner, D. A.; Abraham, C.; Selkoe, D. J. X-ray-Diffraction from Intraneuronal Paired Helical Filaments and Extraneuronal Amyloid Fibers in Alzheimers-Disease Indicates Cross-Beta Conformation. *Proc. Natl. Acad. Sci. U.S.A.* **1986**, *83*, 503−507.

(11) Petkova, A. T.; Ishii, Y.; Balbach, J. J.; Antzutkin, O. N.; Leapman, R. D.; Delaglio, F.; Tycko, R. A Structural Model for Alzheimer's Beta-Amyloid Fibrils Based on Experimental Constraints from Solid State NMR. *Proc. Natl. Acad. Sci. U.S.A.* **2002**, *99*, 16742−16747.

(12) Luhrs, T.; Ritter, C.; Adrian, M.; Riek-Loher, D.; Bohrmann, B.; Doeli, H.; Schubert, D.; Riek, R. 3D Structure of Alzheimer's Amyloid-beta(1−42) Fibrils. *Proc. Natl. Acad. Sci. U.S.A.* **2005**, *102*, 17342−17347.

(13) Kayed, R.; Head, E.; Thompson, J. L.; McIntire, T. M.; Milton, S. C.; Cotman, C. W.; Glabe, C. G. Common Structure of Soluble Amyloid Oligomers Implies Common Mechanism of Pathogenesis. *Science* **2003**, *300*, 486−489.

(14) Caughey, B.; Lansbury, P. T. ProtoFibrils, Pores, Fibrils, and Neurodegeneration: Separating the Responsible Protein Aggregates from the Innocent Bystanders. *Annu. Rev. Neurosci.* **2003**, *26*, 267−298.

(15) Khlistunova, I.; Biernat, J.; Wang, Y.; Pickhardt, M.; von Bergen, M.; Gazova, Z.; Mandelkow, E.; Mandelkow, E. M. Inducible Expression of Tau Repeat Domain in Cell Models of Tauopathy: Aggregation is Toxic to Cells but Can Be Reversed by Inhibitor Drugs. *J. Biol. Chem.* **2006**, *281*, 1205−1214.

(16) Dahlgren, K. N.; Manelli, A. M.; Stine, W. B.; Baker, L. K.; Krafft, G. A.; LaDu, M. J. Oligomeric and Fibrillar Species of Amyloid-Beta Peptides Differentially Affect Neuronal Viability. *J. Biol. Chem.* **2002**, *277*, 32046−32053.

(17) Deshpande, A.; Mina, E.; Glabe, C.; Busciglio, J. Different Conformations of Amyloid Beta Induce Neurotoxicity by Distinct Mechanisms in Human Cortical Neurons. *J. Neurosci.* **2006**, *26*, 6011−6018.

DOI: 10.1021/acs.jpcb.5b00006
J. Phys. Chem. B 2015, 119, 5145−5155

(18) Jeong, J. S.; Ansaloni, A.; Mezzenga, R.; Lashuel, H. A.; Dietler, G. Novel Mechanistic Insight into the Molecular Basis of Amyloid Polymorphism and Secondary Nucleation During Amyloid Formation. *J. Mol. Biol.* **2013**, *425*, 1765−1781.
(19) Morris, R. J.; Eden, K.; Yarwood, R.; Jourdain, L.; Allen, R. J.; Macphee, C. E. Mechanistic and Environmental Control of the Prevalence and Lifetime of Amyloid Oligomers. *Nat. Commun.* **2013**, *4*, 1891.
(20) De Felice, F. G.; Ferreira, S. T. Beta-Amyloid Production, Aggregation, and Clearance as Targets for Therapy in Alzheimer's Disease. *Cell. Mol. Neurobiol.* **2002**, *22*, 545−563.
(21) Roberson, E. D.; Scearce-Levie, K.; Palop, J. J.; Yan, F.; Cheng, I. H.; Wu, T.; Gerstein, H.; Yu, G. Q.; Mucke, L. Reducing Endogenous Tau Ameliorates Amyloid Beta-Induced Deficits in an Alzheimer's Disease Mouse Model. *Science* **2007**, *316*, 750−754.
(22) Wang, S. S.; Liu, K. N.; Han, T. C. Amyloid Fibrillation and Cytotoxicity of Insulin are Inhibited by the Amphiphilic Surfactants. *Biochim. Biophys. Acta* **2010**, *1802*, 519−530.
(23) Morgan, C.; Bugueno, M. P.; Garrido, J.; Inestrosa, N. C. Laminin Affects Polymerization, Depolymerization and Neurotoxicity of Abeta Peptide. *Peptides* **2002**, *23*, 1229−1240.
(24) Svennerholm, L. Gangliosides-a new Therapeutic Agent Against Stroke and Alzheimer's Disease. *Life Sci.* **1994**, *55*, 2125−2134.
(25) Castillo, G. M.; Ngo, C.; Cummings, J.; Wight, T. N.; Snow, A. D. Perleacan Binds to the Beta-Amyloid Proteins (Aβ) of Alzheimer's Disease, Accelerate Aβ Fibril Formation, and Maintains Aβ Fibril Stability. *J. Neurochem.* **1997**, *69*, 2452−2465.
(26) Antosova, A.; Chelli, B.; Bystrenova, E.; Siposova, K.; Valle, F.; Imrich, J.; Vilkova, M.; Kristian, P.; Biscarini, F.; Gazova, Z. Structure-Activity Relationship of Acridine Derivatives to Amyloid Aggregation of Lysozyme. *Biochim. Biophys. Acta* **2011**, *1810*, 465−474.
(27) Gazova, Z.; Bellova, A.; Daxnerova, Z.; Imrich, J.; Kristian, P.; Tomascikova, J.; Bagelova, J.; Fedunova, D.; Antalik, M. Acridine Derivatives Inhibit Lysozyme Aggregation. *Eur. Biophys. J.* **2008**, *37*, 1261−1270.
(28) Vuong, Q. V.; Siposova, K.; Nguyen, T. T.; Antosova, A.; Balogova, L.; Drajna, L.; Imrich, J.; Li, M. S.; Gazova, Z. Binding of Glyco-Acridine Derivatives to Lysozyme Leads to Inhibition of Amyloid Fibrillization. *Biomacromolecules* **2013**, *14*, 1035−1043.
(29) Gazova, Z.; Siposova, K.; Kurin, E.; Mucaji, P.; Nagy, M. Amyloid Aggregation of Lysozyme: The Synergy Study of Red Wine Polyphenols. *Proteins* **2013**, *81*, 994−1004.
(30) Yatin, S. M.; Yatin, M.; Varadarajan, S.; Ain, K. B.; Butterfield, D. A. Role of spermine in Amyloid Beta-Peptide-Associated Free Radical-Induced Neurotoxicity. *J. Neurosci. Res.* **2001**, *63*, 395−401.
(31) Dolphin, G. T.; Chierici, S.; Ouberai, M.; Dumy, P.; Garcia, J. A Multimeric Quinacrine Conjugate as a Potential Inhibitor of Alzheimer's Beta-Amyloid Fibril Formation. *ChemBioChem.* **2008**, *9*, 952−963.
(32) Evans, C. G.; Wisen, S.; Gestwicki, J. E. Heat Shock Proteins 70 and 90 Inhibit Early Stages of Amyloid Beta Aggregation in Vitro. *J. Biol. Chem.* **2006**, *281*, 33182−33191.
(33) Bush, A. I. Metal Complexing Agents as Therapies for Alzheimer's Disease. *Neurobiol. Aging* **2002**, *23*, 1031−1038.
(34) Nitz, M.; Fenili, D.; Darabie, A. A.; Wu, L.; Cousins, J. E.; McLaurin, J. Modulation of Amyloid-beta Aggregation and Toxicity by Inosose Stereoisomers. *FEBS J.* **2008**, *275*, 1663−1674.
(35) Takahashi, T.; Tada, K.; Mihara, H. RNA Aptamers Selected Against Amyloid Beta-Peptide (Aβ) Inhibit the Aggregation of Aβ. *Mol. BioSyst.* **2009**, *5*, 986−991.
(36) Cummings, J. L. Alzheimer's Disease. *N. Engl. J. of Med.* **2004**, *351*, 56−67.
(37) Hawkes, C. A.; Vivian, N.; MacLaurin, J. Small Molecule Inhibitors of Aβ-aggregation and Neurotoxity. *Drug Dev. Res.* **2009**, *70*, 111−124.
(38) Yamin, G.; Ono, K.; Inayathullah, M.; Teplow, D. B. Amyloid β-Protein Assembly as Therapeutic Target of Alzheimer's Disease. *Curr. Pharm. Des.* **2008**, *14*, 3231−3246.
(39) Huy, P. D. Q.; Yu, Y.-C.; Ngo, S. T.; Thao, T. V.; Chen, C.-P.; Li, M. S.; Chen, Y.-C. In Silico and in Vitro Characterization of Anti-Amyloidogenic Activity of Vitamin K3 Analogues for Alzheimer's Disease. *Biochim. Biophys. Acta, Gen. Subjects* **2013**, *1380*, 2960−2969.
(40) Oken, B. S.; Storzbach, D. M.; Kaye, J. The Efficacy of Ginkgo Biloba on Cognitive Function in Alzheimer Disease. *Arch Neurol.* **1998**, *55*, 1409−1415.
(41) Ngo, S. T.; Li, M. S. Top-Leads From Natural Products for Treatment of Alzheimer's Disease: Docking and Molecular Dynamics Study. *Mol. Simul.* **2013**, *39*, 279−291.
(42) Viet, M. H.; Chen, C. Y.; Hu, C. K.; Chen, Y. R.; Li, M. S. Discovery of Dihydrochalcone as Potential Lead for Alzheimer's Disease: in Silico and in Vitro Study. *PLoS One* **2013**, *8*, e79151.
(43) Sciarretta, K. L.; Gordon, D. J.; Meredith, S. C. Peptide-Based Inhibitors of Amyloid Assembly. *Methods Enzymol.* **2006**, *413*, 273−312.
(44) Hard, T.; Lendel, C. Inhibition of Amyloid Formation. *J. Mol. Biol.* **2012**, *421*, 441−465.
(45) Tjernberg, L. O.; Naslund, J.; Lindqvist, F.; Johansson, J.; Karlstrom, A. R.; Thyberg, J.; Terenius, L.; Nordstedt, C. Arrest of Beta-Amyloid Fibril Formation by a Pentapeptide Ligand. *J. Biol. Chem.* **1996**, *271*, 8545−8548.
(46) Soto, C. M.; Kindy, S.; Baumann, M.; Frangione, B. Inhibition of Alzheimer's Amyloidosis by Peptides that Prevent β-Sheet Conformation. *Biochem. Biophys. Res. Commun.* **1996**, *226*, 672−680.
(47) Adessi, C.; Soto, C. Beta-Sheet Breaker Strategy for the Treatment of Alzheimer's Disease. *Drug Dev. Res.* **2002**, *56*, 184−193.
(48) Li, H. Y.; Monien, M. B.; Lomakin, A.; Zemel, R.; Fradinger, E. A.; Tan, M. A.; Spring, S. M.; Urbanc, B.; Xie, C. W.; Benedek, G. B.; et al. Mechanistic Investigation of the Inhibition of Aβ_{42} Assembly and Neurotoxicity by Aβ_{42} C-Terminal. *Biochemistry* **2010**, *49*, 6358−6364.
(49) Li, H. Y.; Monien, M. B.; Urbanc, E. A. F. B.; Bitan, G. Biophysical Characterization of Aβ_{42} C-Terminal Fragments: Inhibitors of Aβ_{42} Neurotoxicity. *Biochemistry* **2010**, *49*, 1259−1267.
(50) Wu, C.; Murray, M. M.; Summer, S. L. B. L.; Condron, M. M.; Bitan, G.; Shea, J. E.; Bowers, M. T. The Structure of Aβ_{42} C-terminal Fragments Probed by a Combined Experimental and Theoretical Study. *J. Mol. Biol.* **2009**, *387*, 492−501.
(51) Hilbich, C.; Kisterswoike, B.; Reed, J.; Masters, C. L.; Beyreuther, K. Substitutions of Hydrophobic Amino-Acids Reduce the Amyloidogenicity of Alzheimers-Disease Beta-A4 Peptides. *J. Mol. Biol.* **1992**, *228*, 460−473.
(52) Soto, C.; Sigurdsson, E. M.; Morelli, L.; Kumar, R. A.; Castano, E. M.; Frangione, B. Beta-Sheet Breaker Peptides Inhibit Fibrillogenesis in a Rat Brain Model of Amyloidosis: Implications for Alzheimer's Therapy. *Nat. Med.* **1998**, *4*, 822−826.
(53) Wood, S. J.; Wetzel, R.; Martin, J. D.; Hurle, M. R. Prolines and Amyloidogenicity in Fragments of the Alzheimers Peptide Beta/A4. *Biochemistry* **1995**, *34*, 724−730.
(54) Sawaya, M. R.; Sambashivan, S.; Nelson, R.; Ivanova, M. I.; Sievers, S. A.; Apostol, M. I.; Thompson, M. J.; Balbirnie, M.; Wiltzius, J. J. W.; McFarlane, H. T.; et al. Atomic Structures of Amyloid Cross-Beta Spines Reveal Varied Steric Zippers. *Nature* **2007**, *447*, 453−456.
(55) Sievers, S. A.; Karanicolas, J.; Chang, H. W.; Zhao, A.; Jiang, L.; Zirafi, O.; Stevens, J. T.; Munch, J.; Baker, D.; Eisenberg, D. Structure-Based Design of Non-Natural Amino-Acid Inhibitors of Amyloid Fibril Formation. *Nature* **2011**, *475*, 96−U117.
(56) Lipinski, C. A.; Lombardo, F.; Dominy, B. W. Experimental and Computational Approaches to Estimate Solubility and Permeability in Drug Discovery and Development Settings. *Adv. Drug. Delivery Rev.* **1997**, *23*, 3−25.
(57) Kollman, P. A.; Massova, I.; Reyes, C.; Kuhn, B.; Huo, S.; Chong, L.; Lee, M.; Lee, T.; Duan, Y.; Wang, W.; et al. Calculating Structures and Free Energies of Complex Molecules: Combining Molecular Mechanics and Continuum Models. *Acc. Chem. Res.* **2000**, *33*, 889−897.
(58) Petkova, A. T.; Yau, W. M.; Tycko, R. Experimental Constraints on Quaternary Structure in Alzheimer's β-Amyloid Fibrils. *Biochemistry* **2006**, *45*, 498−512.

DOI: 10.1021/acs.jpcb.5b00006
J. Phys. Chem. B 2015, 119, 5145−5155

(59) Bernstein, S. L.; Dupuis, N. F.; Lazo, N. D.; Wyttenbach, T.; Condron, M. M.; Bitan, G.; Teplow, D. B.; Shea, J.-E.; Ruotolo, B. T.; Robinson, C. V.; et al. Amyloid-beta Protein Oligomerization and the Importance of Tetramers and Dodecamers in the Aetiology of Alzheimer's Disease. *Nat. Chem.* **2009**, *1*, 326−331.
(60) Hayden, E. Y.; Teplow, D. B. Amyloid Beta-Protein Oligomers and Alzheimer's Disease. *Alzheimers Res. Ther.* **2013**, *5*, 60.
(61) Case, D. A., Darden, T. A., Cheatham, T. E., Simmerling, C. L., Wang, J., Duke, R. E., Luo, R., Crowley, M., Walker, R. C., Zhang, W. et al. *AMBER 11*; University of California, San Francisco: San Francisco, CA, 2010.
(62) Alexey Onufriev, D. B.; Case, D. A. Exploring Protein Native States and Large-Scale Conformational Changes with a Modified Generalized Born Model. *PROTEINS* **2004**, *55*, 383−394.
(63) Sanner, M. F. Python: A Programming Language for Software Intergration and Development. *J. Mol. Graphics Modell.* **1999**, *17*, 57−61.
(64) Trott, O.; Olson, A. J. Improving the Speed and Accuracy of Docking with a New Scoring Function, Efficient Optimization, and Multithreading. *J. Comput. Chem.* **2010**, *31*, 455−461.
(65) Shanno, D. F. Conditioning of Quasi-Newton methods for Function Minimization. *Math. Comput.* **1970**, *24*, 647−656.
(66) Darden, T.; York, D.; Pedersen, L. Particle mesh Ewald: An Nlog(N) method for Ewald Sums in Large Systems. *J. Chem. Phys.* **1993**, *98*, 10089−10092.
(67) Hockney, R. W.; Goel, S. P.; Eastwood, J. Quit High Resolution Computer Models of Plasma. *J. Comput. Phys.* **1974**, *14*, 148−158.
(68) Berendsen, H. J. C.; Postma, J. P. M.; van Gunsteren, W. F.; Dinola, A.; Haak, J. R. Molecular Dynamics with Coupling to an External Bath. *J. Chem. Phys.* **1984**, *81*, 3684−3690.
(69) Parrinello, M.; Rahman, A. Polymorphic Transitions in Single Crystals: A New Molecular Dynamics Method. *J. Appl. Phys.* **1981**, *52*, 7182−7190.
(70) Hornak, V.; Abel, R.; Okur, A.; Strockbine, B.; Roitberg, A.; Simmerling, C. Comparison of Multiple Amber Force Fields and Development of Improved Protein Backbone Parameters. *PROTEINS: Struct. Funct. Gen* **2006**, *65*, 712−725.
(71) Jorgensen, W. L.; Chandrasekhar, J.; Madurai, J. D.; Impey, R. W.; Klein, M. L. Comparison of Simple Potential Functions for Simulating Liquid Water. *J. Chem. Phys.* **1983**, *79*, 926−935.
(72) Hess, B.; Kutzner, C.; van der Spoel, D.; Lindahl, E. GROMACS 4: Algorithms for Highly Efficient,Load-Balanced, and Ccalable Molecular Simulation. *J. Chem. Theor. Comput.* **2008**, *4*, 435−447.
(73) Nguyen, T. T.; Viet, M. H.; Li, M. S. Effects of Water Models on Binding Affinity: Evidence from All-Atom Simulation of Binding of Tamiflu to A/H5N1 Neuraminidase. *ScientificWorldJournal* **2014**, *2014*, 536084.
(74) Ngo, S. T.; Li, M. S. Curcumin Binds to Aβ_{1-40} Peptides and Fibrils Stronger than Ibuprofen and Naproxen. *J. Phys. Chem. B* **2012**, *116*, 10165−10175.
(75) Viet, M. H.; Ngo, S. T.; Lam, N. S.; Li, M. S. Inhibition of Aggregation of Amyloid Peptides by Beta-sheet Breaker Peptides and Their Binding Affinity. *J. Phys. Chem. B* **2011**, *115*, 7433−7446.
(76) Nguyen, T. T.; Mai, B. K.; Li, M. S. Study of Tamiflu Sensitivity to Variants of A/H5N1 Virus Using Different Force Fields. *J. Chem. Info. Model.* **2011**, *51*, 2266−2276.
(77) McQuarrie, D. A. *Statistical Thermodynamics*, 2nd ed.; Harper and Row: New York, 1973.
(78) Kuntz, I. D.; Chen, K.; Sharp, K. A.; Kollman, P. A. The Maximal Affinity of Ligands. *Proc. Natl. Acad. Sci. U.S.A.* **1999**, *96*, 9997−10002.
(79) Ritchie, T. J.; Macdonald, S. J. F. The Impact of Aromatic Ring Count on Compound Developability - are too many Aromatic Rings a Liability in Drug Design? *Drug Discovery Today* **2009**, *14*, 1011−1020.
(80) Singh, R. K.; Singh, A.; Singh, D. QSAR Study of Testosterone Derivatives Using Quantum Chemical and Topological Descriptors. *Int. J. Life Sci. Pharma Res.* **2011**, *1*, 52−58.
(81) Roy, K. QSAR of Adenosine Receptor Antagonists II: Exploring Physicochemical Requirements for Selective Binding of 2-Arylpyrazolo[3,4-c]quinoline Derivatives with Adenosine A1 and A3 Receptor Subtypes. *QSAR Comb. Sci.* **2003**, *22*, 614−621.
(82) Hansch, C.; Garg, R.; Kurup, B.; Mekapati, S. B. Allosteric Interactions and QSAR: On the Role of Ligand Hydrophobicity. *Bioorg. Med. Chem.* **2003**, *11*, 2075−2084.
(83) Chou, P. Y.; Fasman, G. D. Conformational Parameters for Amino Acids in Helical, β-sheet, and Random Coil Regions Calculated from Proteins. *Biochemistry* **1974**, *13*, 211−222.
(84) Chou, P. Y.; Fasman, G. D. Empirical Predictions of Protein Conformation. *Annu. Rev. Biochem.* **1978**, *47*, 251−257.
(85) Li, S. C.; Goto, N. K.; Williams, K. A.; Derer, C. M. α-helical, but not β-sheet Propensity of Proline is Determined by Peptide Environment. *Proc. Natl. Acad. Sci. U.S.A.* **1996**, *93*, 6676−6681.
(86) Yang, F.; Lim, G. P.; Begum, A. N.; Ubeda, O. J.; Simmons, M. R.; Ambegaokar, S. S.; Chen, P. P.; Kayed, R.; Glabe, C. G.; Frautschy, S. A.; et al. Curcumin Inhibits Formation of Amyloid β Oligomers and Fibrils, Binds Plaques, and Reduces Amyloid in Vivo. *J. Biol. Chem.* **2005**, *280*, 5892−5901.
(87) Ono, K.; Hasegawa, K.; Naiki, H.; Yamada, M. Curcumin has Potent Anti-Amyloidogenic Effects for Alzheimer's β-Amyloid Fibrils in Vitro. *J. Neurosci. Res.* **2004**, *75*, 742−750.
(88) Khurana, R.; Uversky, V. N.; Nielsen, L.; Fink, A. L. Is Congo Red an Amyloid-specific Dye? *J. Biol. Chem.* **2001**, *276*, 22715−22721.
(89) Tjernberg, L. O.; Lilliehook, C.; Callaway, D. J. E.; Naslund, J.; Hahne, S.; Thyberg, J.; Terenius, L.; Nordstedt, C. Controlling Amyloid Beta-Peptide Fibril Formation with Protease-Stable Ligands. *J. Biol. Chem.* **1997**, *272*, 12601−12605.
(90) Azriel, R.; Gazit, E. Analysis of the Minimal Amyloid-Forming Fragment of the Islet Amyloid Polypeptide. An Experimental Support for the Key Role of the Phenylalanine Residue in Amyloid Formation. *J. Biol. Chem.* **2001**, *276*, 34156−34161.

DOI: 10.1021/acs.jpcb.5b00006
J. Phys. Chem. B 2015, 119, 5145−5155